Impact of composition on the crystal texture and on the dynamics of P(THF-*co*-ECH) copolymers

Jon Maiz[1,2*], *Ester* Verde-Sesto[1], *Isabel* Asenjo-Sanz[1], *Fanni* Juranyi[3], *José A.* Pomposo[1,2,4], *Arantxa* Arbe[1], and *Juan* Colmenero[1,4,5]

[1]Centro de Física de Materiales (CFM) (CSIC-UPV/EHU)-Materials Physics Center (MPC), Paseo Manuel de Lardizábal 5, 20018 Donostia-San Sebastián, Spain
[2]IKERBASQUE-Basque Foundation for Science, Plaza Euskadi 5, 48009 Bilbao, Spain
[3]Laboratory for Neutron Scattering, Paul Scherrer Institut, CH-5232 Villigen, Switzerland
[4]Departamento de Polímeros y Materiales Avanzados: Física, Química y Tecnología, Universidad del País Vasco-Euskal Herriko Unibertsitatea (UPV/EHU), 20018 Donostia-San Sebastián, Spain
[5]Donostia International Physics Center, Paseo Manuel de Lardizábal 4, 20018, Donostia-San Sebastián, Spain

Abstract. We present a combined study by quasielastic neutron scattering (QENS), differential scanning calorimetry (DSC) and wide angle X-ray scattering (WAXS) on poly(tetrahydrofuran-co-epichlorohydrin) copolymers, to see how their composition can be used to tune their crystallizability and to elucidate the impact of this factor on the dynamical properties. QENS reveals a strong effect on the local dynamics upon cooling down, where the local motions of a sample that remains in the supercooled state at lower temperatures are less Gaussian and slower than those in a sample that crystallizes a few degrees below. This can be attributed to the enhancement of local heterogeneities in the former, which could be a determining factor preventing crystallization.

1 INTRODUCTION

The structure of polymer materials is dictated by the crystallization and chain organization, and, in general, these two factors are important to understand the final properties of the system. In industry, during the last years multiphasic polymer materials have been developed in order to reach suitable final properties with the aim of extend them in different fields. To achieve this goal, researchers are trying to implement and/or develop new multiphasic polymers or complex systems, among them, polymer blends, polymer composites (or nanocomposites), polymer gels and different types of copolymers [1].

One of the most common type of copolymers are random copolymers. This type of copolymers are characterized by a statistical order of the repeating units along the backbone of the chain. The main objective of the synthesis of this kind of polymers is to achieve a homogeneous system with tunable properties depending on their composition. In the case of random copolymers, an average in the physical and chemical properties is observed e. g. in the value of the glass transition temperature (T_g). Moreover, random copolymers display a single-phase morphology; the sequences are normally too short to induce a phase separation morphology.

Over last years our group has developed different works related with poly(tetrahydrofuran-*co*-epichlorohydrin) P(THF-*co*-ECH) copolymers [2-5]. The main motivation of this interest was to produce functionalized linear chains to be used as precursors for the synthesis of Single Chain Nano-Particles (SCNPs); therefore, along this work, we will use the term 'precursor' to refer to these polymers. Polymer melts in general are complex systems where the relevant dynamic processes depend on the length scale of observation [6,7]. The dynamics is naturally intrinsically connected to the structural properties of the system. In the case of the copolymers here investigated, their composition can be used to tune their crystallizability. While PTHF has a strong tendency to cristallize, PECH is easily obtained in the glassy state upon cooling. Precursors rich in THF comonomer could form crystalline phases. Semicrystalline polymers have a partial regular chain structure, where the regular part is able to crystallize and the irregular part remains in the amorphous state. The crystalline part can adapt its conformation to the lowest energy state forming the denominated crystal whereas the chain defects are normally confined in the amorphous region [8,9]. It is well known that crystallinity of polymeric materials largely affects the properties of the remaining amorphous phase, in terms of structure and dynamics. Many questions remain unsolved in this type of semicrystalline polymers or complex systems. In this context, scattering techniques and particularly neutron scattering techniques are especially appropriate. Neutron scattering encompasses a set of non-destructive experimental techniques that enable the molecular

* Corresponding author: jon.maizs@ehu.eus

analysis of complex systems over a broad range of length and time scales.

In the present work, we investigate the impact of the composition on the crystallization process and on the obtained structural arrangements of bulk systems of precursor chains containing different relative amounts of ECH and THF monomers in the chains. We have explored a sample with a low amount of ECH content, c_{ECH} = 13% (ePrec), where the presence of THF leads to crystalline portions in material, and a sample with higher amount of ECH content, c_{ECH} of 27% (EPrec), that remains amorphous upon cooling. Differential Scanning Calorimetry (DSC) and Wide Angle X-Ray Scattering (WAXS) techniques are used to investigate these features. In addition, we carried out QENS experiments to study the incoherent scattering function of the hydrogens in both samples. For this investigation, a time-of flight (ToF) spectrometer was used in order to determine the segmental relaxation in both samples.

2 EXPERIMENTAL SECTION

2.1 Materials

All reagents and solvents were purchased from Merck (Munich, Germany) and Scharlab (Barcelona, Spain). Tetrahydrofuran (THF, ≥ 99.9% (GC), from Scharlab) was dried using calcium hydride as drying agent (CaH_2, 95 % from Merck, Aldrich), degassed by three freeze-degas-thaw cycles and distilled under reduce pressure at 323 K. The purification of (±)-Epichlorohydrin (ECH, ≥ 99 % (GC) from Merck, Aldrich) was performed by distillation under reduced pressure at 323 K. Tris(pentafluorophenyl)borane ($B(C_6F_5)_3$, 95 %, from Merck, Aldrich) was purified by sublimation under reduce pressure at 333 K using a cold finger condenser. Anhydrous N,N-dimethylformamide (DMF, ≥ 99.8 %, Scharlab), sodium azide (NaN_3, ≥ 99.5 % from Merck, Aldrich), and methanol (MeOH, ≥ 99.9%, Scharlab) were used as received.

2.2 Synthesis Methods

Synthesis of THF and ECH copolymers (P(THF-co-ECH)): Two copolymers of THF and ECH (amorphous and semicrystalline) were synthesized following a similar synthetic procedure previously described by our group [10]. Both polymerization reactions were carried out in bulk and under argon atmosphere. Amorphous P(THF-*co*-ECH): $B(C_6F_5)_3$ (200 mg, 0.4 mmol), THF (25.0 mL, 308.0 mmol) and ECH (6.3 mL, 81.0 mmol) were added into a Schlenk flask of 100 mL. Then, the mixture of reaction was stirred at room temperature (r.t.) for 48 h. The crude product of the reaction was precipitated three times in cold MeOH (3 x 600 mL) in order to remove unreacted monomers. The obtained copolymer was dried at 313 K under vacuum for 24 h, producing a sticky transparent material (P(THF-*co*-ECH, 22.1 g, 74 % of yield). The ECH content was determined by 1H Nuclear Magnetic Resonance (1H NMR) and estimated to be 27 mol %. By Size-Exclusion Chromatography (SEC), M_w = 38 kg/mol with polydispersity Đ = M_w/M_n = 1.27 were determined. The preparation of P(THF-*co*-ECH) semicrystalline was carried out following a procedure similar to that described above but with a different ratio of reagents: $B(C_6F_5)_3$ (44 mg, 0.09 mmol), THF (12.5 mL, 154.00 mmol) and ECH (1.33 mL, 17.1 mmol). We obtained 9.5g of copolymer, 75 % of yield. 1H NMR: 13 % ECH. SEC: 48 kg/mol, Đ = 1.32.

Synthesis of the azide-containing precursors (EPrec and ePrec) by azidation of the obtained P(THF-*co*-ECH)s: a solution of 2.0 g of P(THF-*co*-ECH) in 80 mL of anhydrous DMF was prepared into a round-bottom flask of 500 mL. Then, NaN_3 (925 mg) was added into the solution, and the obtained suspension was stirred for 24 h at 333 K. The mixture of the reaction was filtrated to remove NaCl generated and the unreacted NaN_3 and evaporated under reduced pressure until to get ca 15 mL. Then, the resulting crude product was precipitated in a cold mixture of 200 mL of 1:4 H_2O/MeOH and dried at 313 K under vacuum for 24 h to obtain the precursor (EPrec: 1.5 g, 72 % yield). The molecular weight M_w was 38.5 kg/mol with polydispersity Đ = M_w/M_n of 1.23 (determined by Size-Exclusion Chromatography (SEC)). Composition by elemental analysis (EA) calculated: C (%) cal. 58.94, H (%) cal. 9.61, N (%) cal. 3.36 and composition by EA found: C (%) exp. 58.56, H (%) exp. 9.88, N (%) exp. 3.81. The synthesis of ePrec was carried out following the same synthetic procedure described for EPrec: 2.5g of P(THF-*co*-ECH) crystalline, 100 mL of DMF and 0.65 g of NaN_3. We obtained 2.1 g of ePrec, 84% of yield. SEC: 47.5 kg/mol, Đ = 1.32. Composition by EA calculated: C (%) cal. 61.89, H (%) cal. 10.14, N (%) cal. 2.41 and composition by EA found: C (%) exp. 61.43, H (%) exp. 10.18, N (%) exp. 2.53.

2.3 Sample Preparation

Two different precursor bulk samples were studied in this work, EPrec and ePrec. For neutron scattering experiments, first solutions containing the sample and 2 mL of CH_2Cl_2 were stirred until completed dissolution, and then solutions were drop-casted onto the aluminum flat holders. Finally the solvent was completely evaporated, first slowly in the fume hood and subsequently in an oven under vacuum conditions at 343 K for 24 h.

2.4 Thermal Analysis

Calorimetric values were studied by differential scanning calorimetry (DSC). A TA instruments Q2000 under ultrapure nitrogen flow was used to carried out the DSC experiments. The protocol followed for each sample was: first, the samples were heated up until 350 K and kept at this temperature for 3 min in order to erase any previous thermal history. Thereafter, they were cooled down until 170 K and subsequently they were again heated up until 350 K. The cooling and heating rate used in the whole procedure was 20 K/min. Around 5 mg of the polymer mass was used in each sample.

2.5 Structural Analysis

Wide angle X-ray scattering (WAXS) technique on a Bruker D8 Advance diffractometer equipment was used to study the short-range order of the systems. The equipment works in parallel beam geometry with CuK_α transition photons of wavelength λ = 1.54 Å, in reflection mode (θ - 2θ configuration). The scattering angle 2θ was varied from 10º to 30º with steps of 0.05º. Two different temperatures were explored, at 233 and 300 K. The scattered intensities were recorded as a function of the scattering vector Q, $Q = 4\pi\lambda^{-1} \sin\theta$.

2.6 Quasielastic Neutron Scattering (QENS) Analysis

The QENS experiments were carried out on the SINQ time-of-flight FOCUS spectrometer. An incident wavelength of 6 Å was used yielding an energy resolution of around 40 μeV. Cuts at constant Q-value were performed in the energy range ±1meV. The effective Q-range covered was between 0.2 and 1.8 $Å^{-1}$. Five different temperatures were studied: 250, 290, 320, 360 and 400 K. A low temperature measurement (~ 40 K) of each sample was used for the accurate normalization of the Fourier transformed and deconvoluted results in each sample. Samples were filling flat aluminum sample holders, and with thicknesses calculated to yield a transmission of 90%.

3 RESULTS

First, in Fig. 1 the calorimetric results are shown.

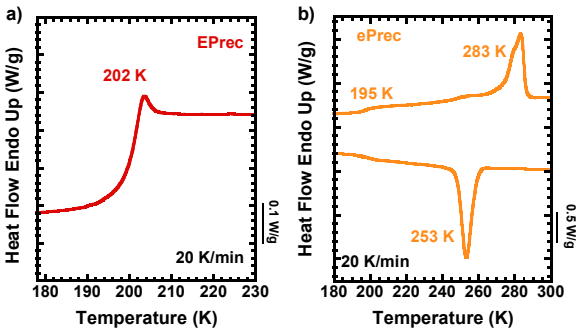

Fig. 1. DSC (a) heating scan for EPrec sample after the previous cooling process and (b) cooling and heating scans for ePrec sample at 20 K/min.

In Fig. 1a the DSC heating scan that corresponds to EPrec is presented. The T_g value calculated from the onset value for this sample is 202 K. Meanwhile, in Fig. 1b for ePrec both cooling and heating scans at 20 K/min are shown. This sample shows a crystallization process occurring at a crystallization temperature T_c of 253 K and a melting process taking place at the melting temperature T_m observed at 283 K. In addition, a T_g value of 195 K can be also estimated for this sample, being this value lower than that obtained for EPrec sample.

The results of the WAXS experiments performed at 233 K and 300 K after a previous cooling scan at 20 K/min in both samples are displayed in Fig. 2. We note that 233 K is below the crystallization temperature for the ePrec sample and 300 K is above the crystallization temperature for the ePrec sample. Both temperatures are above the glass transition temperatures of the samples.

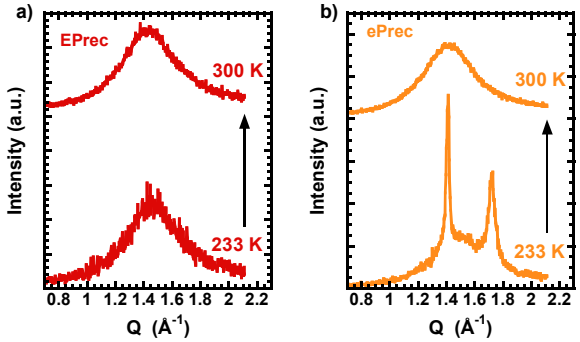

Fig. 2. WAXS measurements at low temperature (233 K) and at room temperature (300 K) for (a) EPrec and (b) ePrec samples after the previous cooling process at 20 K/min.

Fig. 2a shows that there are no appreciable differences on the short-range order for Eprec sample at these temperatures. One main amorphous halo is observed centred at Q ≈ 1.45 $Å^{-1}$, that slightly shifts with increasing temperature towards lower Q-values. This peak is associated with the inter-main chain correlations with average distances of about $d_{chain} = 2\pi/Q_{max} \approx 4.3$ Å. On the other hand, Fig. 2b shows WAXS data that correspond to the ePrec sample at 233 K (below its T_c value) and at 300 K (above its T_m value). The pattern at 233 K shows clear features of crystallinity for the ePrec sample, presenting two main diffraction peaks at 1.41 and 1.72 $Å^{-1}$. When the sample is heated up to 300 K, it melts and only an amorphous halo is observed centred at a similar Q-value as that of the EPrec sample.

If we move to the neutron scattering studies, Fig. 3 shows representative QENS spectra obtained from EPrec and ePrec samples, where the curves are normalized to their value at $\hbar\omega = 0$.

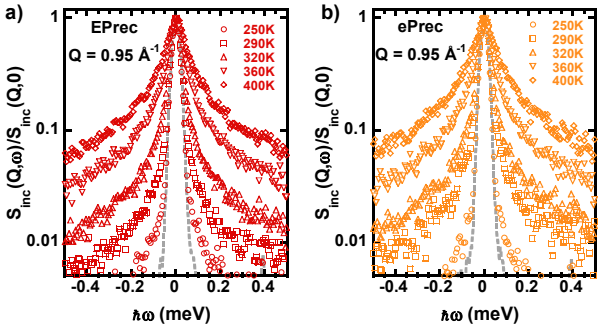

Fig. 3. Normalized FOCUS spectra obtained at Q = 0.95 $Å^{-1}$and the different temperature values indicated for (a) EPrec sample and (b) ePrec sample. The dotted line shows the instrumental resolution function.

The width of the quasielastic spectrum is related to the inverse of the characteristic time of motion probed by the instrument. For all the temperatures studied, at the representative Q-value chosen in Fig. 3 we observe a clear broadening with respect to the instrumental

resolution function. For a given Q-value, this broadening becomes more pronounced with increasing temperature. In Fig. 3b, this increase is more pronounced when the temperature jump is from 250 to 290 K than in Fig. 3a, due to the transition in the ePrec sample from the crystalline material (at 250 K) to its molten state (already at 290 K). As we have confirmed before by DSC data, in Fig. 1b, at this temperature the ePrec sample is already melted (T_m = 283 K).

The spectra measured in the frequency domain are affected by instrumental resolution through convolution. Therefore, the quantitative analysis of the results was performed by Fourier transforming the data to the time domain and deconvoluting them from the instrumental resolution by division. In this way, it is possible to obtain the intermediate incoherent scattering function in the time domain $S_{inc}(Q,t)$. Fig. 4 shows the results obtained from this procedure for EPrec and ePrec samples at the same representative Q-value of 0.95 $Å^{-1}$and at the five different temperatures studied.

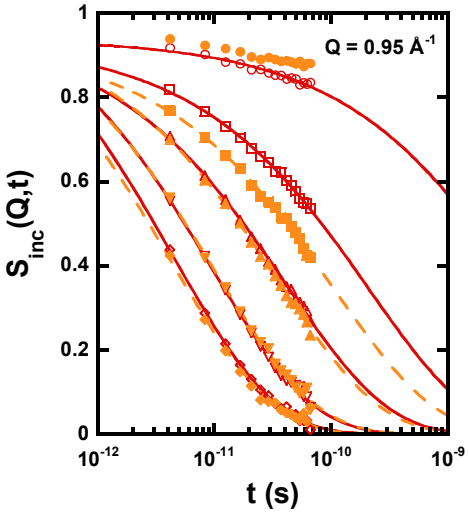

Fig. 4. Fourier-transformed and deconvoluted QENS spectra obtained from FOCUS on EPrec (unfilled) and ePrec (filled) samples at Q-value of 0.95 $Å^{-1}$at the five temperatures investigated: 250 K (circle), 290 K (square), 320 K (up-triangle), 360 K (down-triangle) and 400 K (diamond). Lines are Kohlrausch-Williams-Watts (KWW) fits with β = 0.5.

The QENS results in glass-forming polymers are usually described by Kohlrausch-Williams-Watts (KWW) or stretched exponential functions

$$S_{inc}(Q,t) = A(Q)\exp\left[-\left(\frac{t}{\tau_s}\right)^{\beta}\right] \quad (1)$$

where β is the stretching parameter characterizing the deviations from a single exponential. The prefactor A (Q) accounts for the decay of the correlation function at shorter times due to vibrational and other fast contributions. In Fig. 4 we can observe that the description using Eq. 1 with β = 0.5 works well for both samples in the covered T-range for the Q-value shown. The exception is the sample ePrec at the lowest temperature investigated (250 K), where the tendency toward a plateau-like behaviour at long times prevents fitting with the same functional form as the other curves. At this temperature, the ePrec sample –rich in THF comonomer– is in the semicrystalline form. This behaviour is attributable to the contribution of an elastic fraction reflecting the frozen dynamics of the crystalline portion of the material. Therefore, the KWW function (Eq 1.) was not applied for describing the result at 250 K. Fig. 5 shows the results obtained for EPrec and ePrec samples for four temperatures measured at four different representative Q-values.

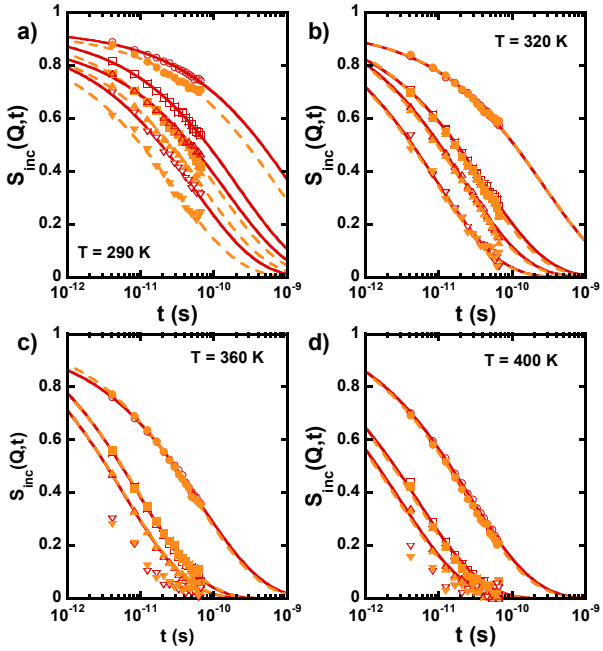

Fig. 5. Fourier-transformed and deconvoluted QENS spectra obtained by FOCUS on EPrec (unfilled) and ePrec (filled) samples at four Q-values investigated: 0.55 $Å^{-1}$ (circle), 0.95 $Å^{-1}$ (square), 1.15 $Å^{-1}$ (up-triangle) and 1.65 $Å^{-1}$ (down-triangle) and at the four temperatures studied: (a) 290 K, (b) 320 K, (c) 360 K and (d) 400 K. Lines are Kohlrausch-Williams-Watts (KWW) fits with β = 0.5.

The results, as can be appreciated in Figs. 4 and 5, can be in general reasonably well described by Eq. 1, using just a constant β-value of 0.5. We note, however, that for high Q-values and temperatures –as it is the case of 1.65 $Å^{-1}$ at 360 and 400 K shown in Fig. 5– the decay of the intermediate scattering function for both samples takes place with very short characteristic times. Actually, the function decays to values smaller than 1/e already at times shorter than 2—3ps. Therefore, we did not consider these results to fit them by KWW functions (we discarded all results which τ_s was smaller than 5ps). From the characteristic times τ_s and stretching parameters β, the average characteristic time can be calculated as $\langle\tau\rangle = \tau_s\Gamma(1/\beta)/\beta$. The results on these characteristic times are displayed in Fig. 6.

For Q-values below 1 $Å^{-1}$, the hydrogen motions in the α-relaxation regime of glass-forming systems usually follow the Gaussian prediction [2,4,5,11-13]. At higher Qs, deviations from this Gaussian behavior are found in general. This is also the case of our samples (see Fig. 6). The dotted line there shows the $\tau \sim Q^{-2/\beta}$ dependence corresponding to the Gaussian prediction in stretched exponential intermediate scattering functions. To account for deviations from the Gaussian

approximation, the jump diffusion model might be invoked in simple systems where diffusion governs at long times [14-16]. This model considers that an atom remains in a given site for a time, τ_0, where it vibrates around a center of equilibrium. After this time τ_0, it moves rapidly to a new position separated from the previous one by the vector $\vec{l}$. This model was extended to the case of subdiffusive behavior by the anomalous jump diffusion (AJD) model [11,12]. The AJD model introduces stretching in the time-dependent part of the intermediate scattering function. In this framework, the KWW function has a characteristic time given by:

$$\tau_s\,(Q) = \tau_{s,0}\left[1 + \frac{1}{Q^2 l_0^2}\right]^{\frac{1}{\beta}} \qquad (2)$$

where l_0 is the preferred jump length and $\tau_{s,0}$ is the time between jumps [12]. The AJD model was used to describe the Q-dependence of the characteristic times obtained for 250 K for EPrec and for T = 320 and 290 K for the two samples, where the values of the AJD parameters could be determined with better accuracy. The values obtained for the parameters are listed in Table 1. For the two highest temperatures investigated, the uncertainties involved in the values of the characteristic times at high-Q –where the intermediate scattering function decays to a large extent due to vibrations and faster processes, as explained above— prevented a precise independent determination of the two parameters $\tau_{s,0}$ and l_0.

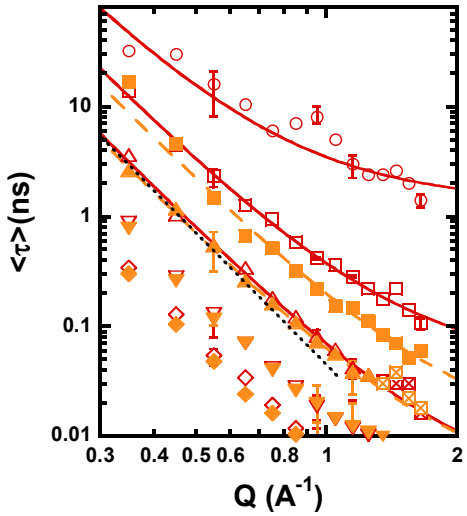

Fig. 6. Average time for H motions obtained for EPrec (unfilled) and ePrec (filled) samples at 250 K (circle), 290 K (square), 320 K (up-triangle), 360 K (down-triangle) and 400 K (diamond), imposing β = 0.5. Lines are fits of Eq. 2 to EPrec (solid lines) and ePrec (dashed lines). The dotted line shows the low-Q Gaussian behavior for the 320 K data. Error bars have been included at selected Q-values (0.55, 0.95, 1.15 and 1.65 $Å^{-1}$). Results at 320 K and high Q-values represented by crossed squares are subject to very large uncertainties and were not considered in the fit.

Table 1. Values of the parameters involved in the Anomalous Jump Diffusion (AJD) fitting the EPrec and ePrec results described with KWW functions.

Sample	T (K)	$\tau_{s,0}$ (ps)	l_0 (Å)
EPrec	250	678±191	1.3±0.19
	290	21±6	0.71±0.07
	320	1.4±0.4	0.50±0.04
ePrec	250	-	-
	290	4.5±1.2	0.52±0.05
	320	1.5±0.4	0.52±0.04

4 DISCUSSION

Combining "macroscopic" and "microscopic" techniques it is possible to investigate how the composition affects the crystallization capability and the dynamics of copolymer systems in the bulk. The calorimetric studies gave us a direct idea of how the comonomer relative content in the chains can affect the crystallinity of the system. Consistent with the DSC results obtained, WAXS experiments also show directly the difference in crystallization tendency of the samples. This crystallinity can be tuned changing the composition in a copolymer, where one of the components is a semicrystalline polymer (PTHF) and the other one is an amorphous material (PECH). When a c_{ECH} of 27 % was used (EPrec), by calorimetry we have demonstrated that the system become amorphous. On the other hand, when a c_{ECH} of 13% is prepared (ePrec), crystallinity persists in the material. The peaks observed by WAXS at 1.41 and 1.72 $Å^{-1}$ are assignable to the (020) and (110) planes of the monoclinic unit cell of PTHF [17], and should thus correspond to THF comonomer. Thus, we could resolve the pure PTHF crystalline structure in the pattern of ePrec. On the other hand, it is found in the literature that the T_m value for the neat PTHF is around 320 K. In the ePrec sample, the T_m value decreases to 283 K. This is the usual behavior observed for this kind of copolymers, that when the relative content of ECH increases, the T_m value decreases until a composition beyond which the copolymer ends up being amorphous (as it is the case of the EPrec sample here investigated).

The insight provided by QENS data on the H-dynamics shows that the composition, determining the amorphous or semicrystalline morphology, has very little influence on the dynamics at temperatures well above the glass transitions. For experiments done from 320 K up to 400 K, the dynamic behaviour is practically independent of the composition, within the experimental uncertainties. Particularly at temperatures higher than 320 K, the deviations from Gaussian behaviour become very difficult to quantify, due to the fast character of the dynamics. On the contrary, composition strongly affects the decay of the intermediate scattering function at temperatures lower than and slightly above the melting point of the crystalline sample (ePrec) with respect to

the amorphous one. At temperatures above but close to the melting point of the crystalline sample (T = 290 K), the atomic motions in the already molten sample are accelerated with respect to the amorphous one (Fig. 4, 5b and 6). This observation is consistent with the lower T_g value observed for the ePrec sample by DSC experiments. These results indicate a lower fragility (in the meaning of Angell [18]) for ePrec.

In terms of the AJD model, we observe longer residence times and larger jump lengths for the EPrec sample than for the molten one (ePrec) at 290 K (see Table 1). This observation could be attributed to a higher degree of heterogeneities in the local atomic displacements induced by the higher amount of ECH monomers in the EPrec sample. We also note that the deviations from Gaussian behaviour observed at 250 K for this sample are very pronounced and characterized by a very large average jump length. At this temperature, the atomic motions in the amorphous portions of the semicrystalline sample ePrec take place within the confined regions imposed by the crystalline regions.

5 CONCLUSIONS

P(THF-*co*-ECH) based copolymers at two different compositions were successfully synthesized. Increasing the relative content of ECH suppresses crystallization as shown by DSC and WAXS experiments. QENS reveals a very similar dynamics at very high temperatures independently of composition, while a strong impact is observed upon cooling down, when approaching the melting point of the sample able to crystallize. In this region, the local motions of the sample that remains in the supercooled state are less Gaussian and slower than those in the sample that crystallizes. This can be attributed to the enhancement of local heterogeneities in the presence of a higher ECH concentration, which could be a determining factor preventing crystallization.

In addition to the interest of this study per se, it will serve as reference for the future investigation of the bulk systems consisting of SCNPs synthesized from these precursor polymers.

We acknowledge the Grant PID2021-123438NB-I00 funded by MCIN/AEI/10.13039/501100011033 and by "ERDF A way of making Europe". We also acknowledge the financial support of Eusko Jaurlaritza, code : IT-1566-22 and from the IKUR Strategy under the collaboration agreement between Ikerbasque Foundation and the Materials Physics Center on behalf of the Department of Education of the Basque Government. The authors would like to express their appreciation and thanks to Dr. Amaia Iturrospe for WAXS measurements.

References

[1] A. Boudenne, L. Ibos, Y. Candau, S. Thomas, *Handbook of multiphase polymer systems* (John Wiley & Sons, 2011)

[2] A. Arbe, J. Rubio, P. Malo de Molina, J. Maiz, J. A. Pomposo, P. Fouquet, S. Prevost, M. Khaneft, J. Colmenero, Journal of Applied Physics **127**, 044305 (2020)

[3] J. Maiz, E. Verde-Sesto, I. Asenjo-Sanz, P. Fouquet, L. Porcar, J. A. Pomposo, P. Malo de Molina, A. Arbe, J. Colmenero, Polymers **13**, 50 (2021)

[4] J. Maiz, E. Verde-Sesto, I. Asenjo-Sanz, P. Malo de Molina, B. Frick, J. A. Pomposo, A. Arbe, J. Colmenero, Polymers **13**, 2316 (2021)

[5] J. Maiz, E. Verde-Sesto, I. Asenjo-Sanz, L. Mangin-Thro, B. Frick, J. A. Pomposo, A. Arbe, J. Colmenero, Macromolecules **55**, 2320 (2022)

[6] M. Rubinstein, R. H. Colby, *Polymer physics* (Oxford university press New York, 2003), Vol. 23

[7] D. Richter, M. Monkenbusch, A. Arbe, J. Colmenero, *Neutron spin echo in polymer systems* (Springer Verlag, Berlin Heidelberg New York, 2005), Vol. 174, Advances in Polymer Sciences

[8] L. Mandelkern, *Crystallization of Polymers: Volume 1: Equilibrium Concepts* (Cambridge University Press, Cambridge, 2002), 2 edn., Vol. 1

[9] L. Mandelkern, *Crystallization of Polymers: Volume 2, Kinetics and Mechanisms* (Cambridge University Press, 2004)

[10] J. Rubio-Cervilla, P. Malo de Molina, B. Robles-Hernández, A. Arbe, A. J. Moreno, A. Alegría, J. Colmenero, J. A. Pomposo, Macromolecular Rapid Communications **40**, 1900046 (2019)

[11] A. Arbe, J. Colmenero, F. Alvarez, M. Monkenbusch, D. Richter, B. Farago, B. Frick, Physical Review Letters **89**, 245701 (2002)

[12] A. Arbe, J. Colmenero, F. Alvarez, M. Monkenbusch, D. Richter, B. Farago, B. Frick, Physical Review E **67**, 051802 (2003)

[13] J. Colmenero, A. Alegria, A. Arbe, B. Frick, Physical Review Letters **69**, 478 (1992)

[14] T. Springer, *Quasielastic neutron scattering for the investigation of diffusive motions in solids and liquids* (Springer-Verlag, Berlin, 1972), Springer Tracts in Modern Physics

[15] K. Singwi, A. Sjölander, Physical Review **119**, 863 (1960)

[16] P. A. Egelstaff, *An Introduction to the Liquid State* (Oxford University Press, New York, 1992)

[17] K. Imada, T. Miyakawa, Y. Chatani, H. Tadokoro, S. Murahashi, Die Makromolekulare Chemie **83**, 113 (1965)

[18] C. A. Angell, Science **267**, 1924 (1995)